Vibrational dynamics of cluster-cluster aggregations

Takamichi Terao, Arifumi Yamaya, and Tsuneyoshi Nakayama
Department of Applied Physics, Hokkaido University, Sapporo 060, Japan
(Received 28 July 1997; revised 29 December 1997)

The vibrational dynamics of diffusion-limited cluster-cluster aggregations (DLCA) and reaction-limited cluster-cluster aggregations (RLCA) are numerically studied. The dependence on particle concentration of the density-density correlation function $g(r)$ and the density of states (DOS) $\mathcal{D}(\omega)$ are investigated. It is shown that the frequency dependence of the DOS depends on a sticking probability of clusters when an aggregate is formed. The spectral dimension $\tilde{d}$ on a three-dimensional system is obtained as $\tilde{d}=1.17\pm0.04$ for DLCA, and $\tilde{d}=1.28\pm0.03$ for RLCA. In addition, the scaling properties for the dynamical structure factor $S(q,\omega)$ taking into account the fractality of the DLCA are argued. [S1063-651X(98)06604-5]

PACS number(s): 61.43.Hv, 63.50.+x, 05.90.+m

I. INTRODUCTION

The aggregation process of small particles has attracted a great deal of interest in the past decade, due to their wide range of practical applications or their own scientific importance [1,2]. There are two types of aggregation. One is the particle-cluster aggregation (DLA) proposed by Witten and Sander [3]. A lot of numerical simulations for the DLA model have revealed complex random-dendritic structures with remarkable scaling and universal properties. The fractal dimension D_f of the DLA is distinctly smaller than the Euclidean dimension d. This is a basic model for a variety of aggregations and other growth processes, in which only one particle is allowed in the vicinity of the growing cluster and all growth originates from a collision between single particle and a cluster. However, these features are unrealistic for many actual colloidal systems. The other is the cluster-cluster aggregation model developed by Meakin [4] and Kolb *et al.* [5]. The cluster-cluster aggregation models describe the sol-gel transition due to a nonequilibrium process, whose underlying mechanism leading to the formation of gel networks had been far from complete. Several models have been proposed to elucidate the formation of the gel network, namely, the kinetic equation approach, the bond-percolation model, and the kinetic aggregation model [6]. Among them, the cluster-cluster aggregation model is the most successful one for understanding the gel formation. If the particle concentration c is larger than a characteristic gel concentration c_g, an aggregate spans a box from edge to edge in three directions. At the gelling threshold ($c\approx c_g$), where an aggregate with the fractal dimension D_f reaches the size L of cubic box, one should have

$$c_g \sim \frac{L^{D_f}}{L^d} \sim L^{-(d-D_f)}. \tag{1}$$

As found by Kolb and Herrmann [7], the gel concentration c_g tends to zero in the $L\to\infty$ limit in this model. Numerical simulations indicate that the fractal dimensions of diffusion-limited cluster-cluster aggregation take values of $D_f=1.44\pm0.03$ for $d=2$ and $D_f=1.78\pm0.06$ for $d=3$, respectively [1].

Many of investigations on the vibrational dynamics for self-similar systems, e.g., for percolating networks, have received much attention in this decade [8,9]. Low-frequency modes for these systems are called fractons, which are strongly localized modes [10,11]. Meanwhile, a lot of experiments have been carried out for silica aerogels to clarify the nature of fracton excitations [12–14]. The dynamical scaling arguments have been applied to discuss the universal properties of these systems [10]. In self-similar systems, the density of states $\mathcal{D}(\omega)$ behaves as

$$\mathcal{D}(\omega)\sim\omega^{\tilde{d}-1}, \tag{2}$$

where $\tilde{d}$ is the spectral dimension. For percolating networks, the value of $\tilde{d}$ is approximately equal to $\tilde{d}=4/3$ in the case of a scalar model, independent of the Euclidean dimensions d. However, there is no theoretical prediction on the value of the spectral dimension $\tilde{d}$ for cluster-cluster aggregations because of its complex structure. In general, excitations in self-similar systems are strongly localized, and should obey the single-length scaling postulate (SLSP). It means that all the physically relevant length scales, such as wavelength $\lambda(\omega)$, scattering length $l_s(\omega)$, or localization length $l_c(\omega)$, scale such as [15,16]

$$\Lambda(\omega)\sim\omega^{-\tilde{d}/D_f}. \tag{3}$$

Based on the SLSP, the dynamical structure factor $S(q,\omega)$ should take the following scaling form with the characteristic length $\Lambda(\omega)$:

$$S(q,\omega)=q^y F[q\Lambda(\omega)], \quad (q\equiv|\mathbf{q}|), \tag{4}$$

where $F(x)$ and y are a scaling function and a scaling exponent, respectively.

In this paper, the vibrational dynamics of cluster-cluster aggregations is numerically studied. We have computed the density-density correlation function $g(r)$ and the density of states (DOS) on cluster-cluster aggregations. From these calculations, the relationship between the structure of the cluster-cluster aggregation and its vibrational dynamics is clarified. We have found that the frequency dependence of the DOS depends on a sticking probability of clusters when

an aggregate is formed. At higher concentrations, the crossover from extended phonons to strongly localized excitations (fractons) is clearly realized in the calculated DOS's. We argue also the scaling properties of the dynamical structure factor $S(q,\omega)$ on $d=3$.

II. MODELS

At first, we describe the formation rules of the cluster-cluster aggregation [4,5,17,18]. There are two different models such as diffusion-limited cluster-cluster aggregation (DLCA) and reaction-limited cluster-cluster aggregation (RLCA), which correspond to fast and slow aggregation processes, respectively. We take the unit $a=1$ for a lattice constant. In this model, N particles are randomly disposed in a cubic box of the size L, where the particle concentration becomes $c \equiv N/L^3$. The ith particle (or cluster) is chosen at random according to the probability $P(n_i,\alpha)$ defined by

$$P(n_i,\alpha) \equiv \frac{n_i^\alpha}{\sum_j n_i^\alpha}, \tag{5}$$

where n_i is the number of particles in the ith cluster, and α is a numerical parameter. The ith cluster is moved by one step along a randomly chosen direction among six directions $(\pm 1,0,0)$, $(0,\pm 1,0)$, $(0,0,\pm 1)$ in a cubic box. If the cluster does not collide with another one, the displacement is performed and the algorithm goes on by choosing again another cluster. If a collision occurs between two clusters, they stick together forming a new large cluster with a sticking probability p, and another cluster is chosen again at random. A sticking probability p is chosen as $p=1$ for the DLCA model [17] and $p \ll 1$ for the RLCA model [18,19]. We neglect rotational diffusions, deformations, as well as all kinds of restructuring effects in this process. This is repeated until a single aggregate is formed (see Fig. 1).

Let us consider the equation of motion for these aggregations, consisting of N particles. The equations of motion are given by

$$m\ddot{u}_i(t) = \sum_j \phi_{ij} u_j(t), \tag{6}$$

where $u_i(t)$ and ϕ_{ij} are the displacement of the particle at the ith site and the force constant between the particles i and j, respectively. In Eq. (6), the force constant ϕ_{ij} is taken to be

$$\phi_{ij} = \begin{cases} z_i, & i=j \\ -1 & \text{nearest neighbor} \\ 0 & \text{otherwise} \end{cases}, \tag{7}$$

where z_i is the coordination number at the site i.

III. NUMERICAL RESULTS

We have formed large-scale cluster-cluster aggregations by means of computer simulations. Periodic boundary conditions are employed in all spatial directions. Figure 2 is a typical example of a $d=3$ DLCA formed on a simple-cubic lattice. The system size of the $d=3$ cluster shown in Fig. 2 is

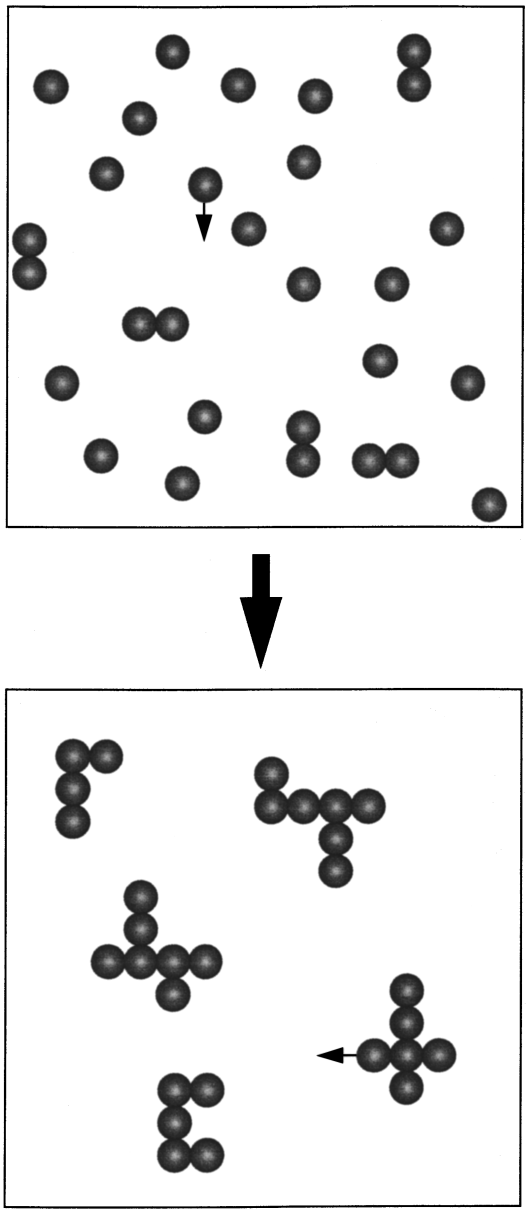

FIG. 1. The formation of the cluster-cluster aggregation.

$L=40$ with the particle concentration $c=0.05$. One can realize that highly ramified structure is formed in a box. The density-density correlation function $g(\mathbf{r})$ is computed to clarify the structure of the DLCA described above. The density-density correlation function $g(\mathbf{r})$ is defined so that $g(\mathbf{r})d\mathbf{r}$ is proportional to a probability of finding a particle in a volume $d\mathbf{r}$ at a distance $\mathbf{r}$ from a given particle. Consequently, for an isotropic material, the number of particle centers (dn) located between r and $r+dr$ from a given particle is proportional to $g(r)4\pi r^2 dr$ in $d=3$. Figure 3(a) shows profiles of $g(r)$ on $d=3$ DLCA for various concentrations. The system size of the DLCA in Fig. 3(a) is taken to be $L=120$. Solid circles, solid triangles, open circles, and open triangles in Fig. 3(a) display the results for $c=0.025$, 0.05, 0.10, and 0.20, respectively. It is shown that the correlation functions $g(r)$ obey the power-law decay for small r. The characteristic length ξ of aggregates is defined as the minimum of $g(r)$ [17]. [See arrows in Fig. 3(a).] For length scale

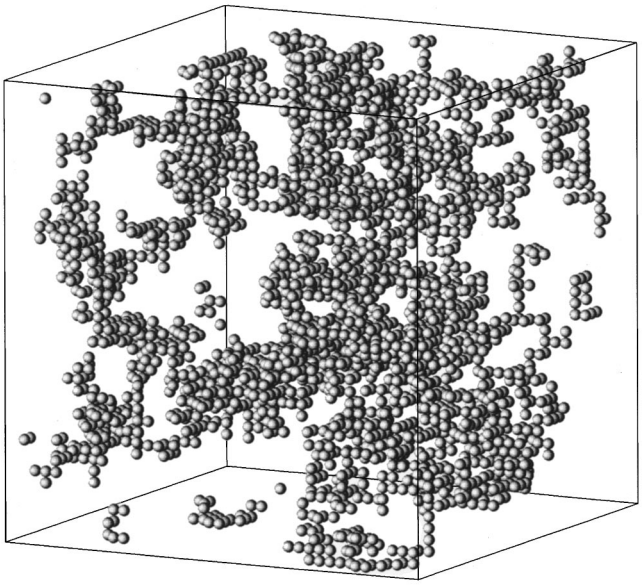

FIG. 2. Three-dimensional ($d=3$) DLCA formed on a simple-cubic lattice. The system size is taken as $L=40$. The particle concentration is $c=0.05$.

$L<\xi$, the system is self-similar (fractal), and for $L>\xi$ the system becomes homogeneous. The dependence of ξ on the concentration c for $d=3$ is shown in the log-log plot in Fig. 3(b). Provided that clusters are fractal with a fractal dimension D_f, one should obtain

$$\xi \sim c^{-1/(d-D_f)} \tag{8}$$

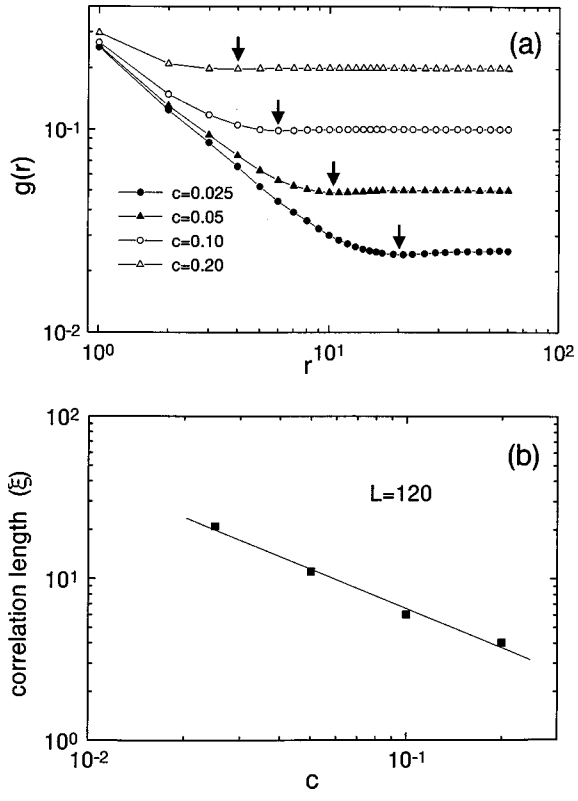

FIG. 3. (a) The density-density correlation function $g(r)$ of $d=3$ DLCA model. The system size is taken as $L=120$. The particle concentration is chosen as $c=0.025$, 0.05, 0.10, and 0.20. (b) The dependence of ξ on the concentration c for $d=3$ DLCA.

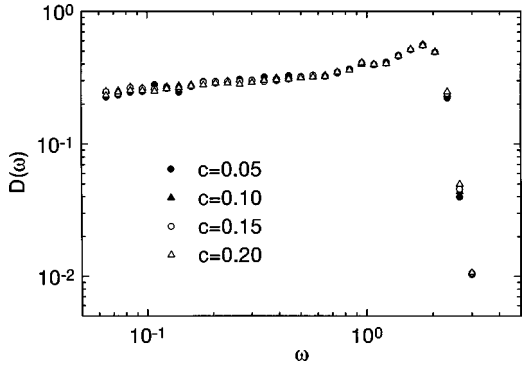

FIG. 4. The vibrational density of states $\mathcal{D}(\omega)$ of $d=2$ DLCA model. The system size is taken as $L=300$. The particle concentration is chosen as $c=0.05$, 0.10, 0.15, and 0.20.

from Eq. (1). A straight-line fitted in Fig. 3(b) gives a slope of -0.81 ± 0.06, leading to $D_f\approx1.77$, in agreement with reported values of $d=3$ DLCA [17].

Vibrational densities of states $\mathcal{D}(\omega)$ of DLCA are calculated using the forced-oscillator method [20,21]. Figure 4 shows vibrational densities of states $\mathcal{D}(\omega)$ of $d=2$ DLCA with different concentrations c under the periodic boundary condition. The system size is taken to be $L=300$, and particle concentrations are given by $c=0.05$, 0.10, 0.15, and 0.20, respectively. The exponent α in Eq. (5) is taken to be $\alpha=0$. The density of states $\mathcal{D}(\omega)$ shows the power-law behavior such as $\mathcal{D}(\omega)\propto\omega^{0.14\pm0.03}$. This power-law behavior reflects the fractal structure of aggregates. We also calculate the DOS for $\alpha=-1/D_f$, which does not make a difference on the frequency dependence of the DOS [22]. From these results, it is shown that the spectral dimension $\tilde{d}$ does not depend on the choice of the exponent α.

Figure 5(a) shows the frequency dependence of the vibrational density of states $\mathcal{D}(\omega)$ of $d=3$ DLCA with different concentrations c. The system size is taken to be $L=160$, which is much larger than that of Ref. [23]. The numbers of particles in DLCA clusters are 102 400, 204 800, 409 600, and 819 200 with the concentration $c=0.025$, 0.05, 0.10, and 0.20, respectively. The ensemble average is taken over 10 samples. At lower concentrations ($c\leqslant0.10$), we find that the frequency dependence of the density of states obeys the power-law behavior $\mathcal{D}(\omega)\propto^{0.17\pm0.04}$. At the higher concentration ($c=0.20$), there is a crossover from the Debye phonon regime ($\propto\omega^2$) to the power-law regime ($\propto\omega^{\tilde{d}-1}$) at the frequency $\omega_c\approx0.02$, where $\tilde{d}$ is the spectral dimension [10]. Our result indicates that the spectral dimension $\tilde{d}$ takes the values $\tilde{d}=1.14\pm0.03$ for $d=2$ DLCA and $\tilde{d}=1.17\pm0.04$ for $d=3$ DLCA, which are distinctly smaller than those for percolating networks ($\tilde{d}\approx4/3$). It is remarkable that the spectral dimensions $\tilde{d}$ of the DLCA do not depend on the Euclidean dimensions d, as in the case of percolating networks [8]. In Fig. 3(a), the correlation length ξ is a few times larger than a lattice constant a at $c=0.10$. It implies that the length scale showing the self-similarity is very small at this concentration. It is surprising that, in spite of the correlation length ξ being very small, the frequency regime where the DOS obeys the power law is quite large at $c=0.10$. We also calculate the DOS of the $d=3$ RLCA model formed on a simple cubic lattice. Figure 5(b) shows the frequency depen-

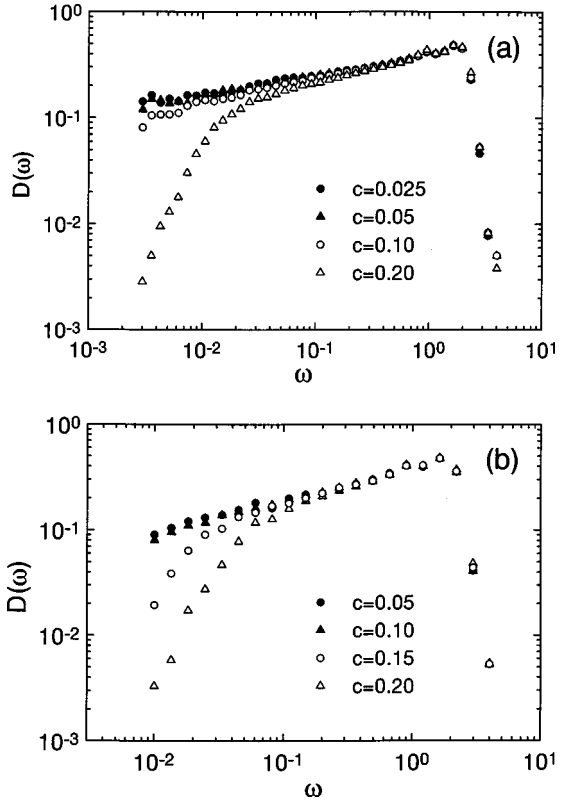

FIG. 5. (a) The vibrational density of states $\mathcal{D}(\omega)$ of $d=3$ DLCA. The system size is taken as $L=160$. The particle concentration is chosen as $c=0.025$, 0.05, 0.10, and 0.20. (b) The vibrational density of states $\mathcal{D}(\omega)$ of $d=3$ RLCA. The system size is taken as $L=80$. The particle concentration is chosen as $c=0.05$, 0.10, 0.15, and 0.20.

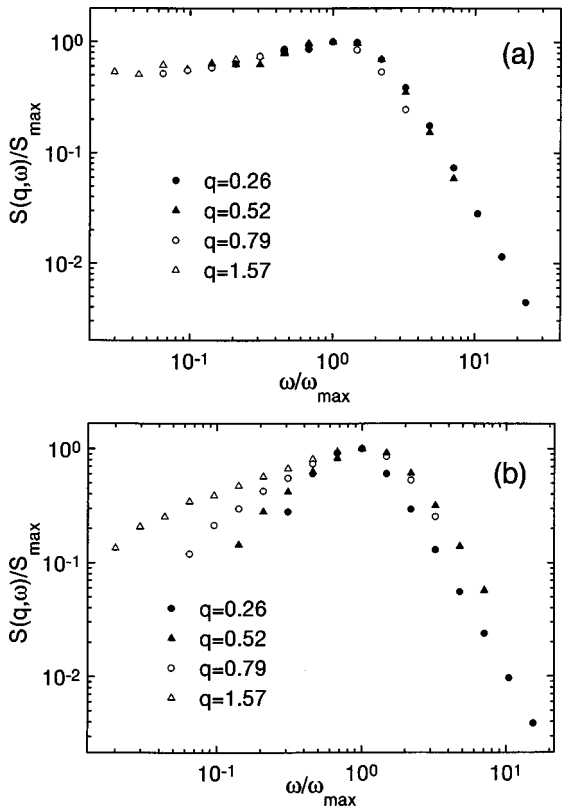

FIG. 6. (a) The rescaled plot of the dynamical structure factor $S(q,\omega)$ of $d=3$ DLCA. The system size is taken as $L=120$. The particle concentration is given by $c=0.025$. (b) The rescaled plot of the dynamical structure factor $S(q,\omega)$ of $d=3$ DLCA. The system size is taken as $L=120$. The particle concentration is given by $c=0.20$.

dence of DOS for four different concentrations, $c=0.05$, 0.10, 0.15, and 0.20. The system size is taken to be $L=80$, and the sticking probability p is chosen to be $p=0.02$ in these calculations. Figure 5(b) indicates that the value of spectral dimension $\tilde{d}$ is equal to $\tilde{d}=1.28\pm0.03$, which is apparently different from that of the DLCA model. It shows that the properties of vibrational dynamics depend on the sticking probability of cluster aggregations on these systems. To our knowledge, this is the first observation of the frequency dependence of DOS on the RLCA model.

Figures 6(a) and 6(b) show the dynamical structure factor $S(\mathbf{q},\omega)$ for $d=3$ DLCA. We have computed the dynamical structure factor $S(\mathbf{q},\omega)$ of $d=3$ DLCA for four different wave vectors $\mathbf{q}$ along the [100] direction. The system size is taken to be $L=120$. A broad peak with a long tail extended to higher frequencies is observed, which qualitatively agrees with the Brillouin spectra of base-catalyzed silica aerogels [24]. Figure 6(a) shows the rescaled plot of the dynamical structure factor $S(q,\omega)$ of $d=3$ DLCA at $c=0.025$. The wave number $q\equiv|\mathbf{q}|$ is taken to be $q=0.26$, 0.52, 0.79, and 1.57. It is shown that the frequency dependence of $S(q,\omega)$ takes a peak value at $\omega=\omega_{\max}$, and $S(q,\omega)$ can be scaled by the frequency $\omega=\omega_{\max}$. The universal curve in Fig. 6(a) exhibits that vibrational excitations on the DLCA satisfy the single-length scaling postulate [15]. The dispersion relation relating the wave number q and the peak position $\omega_{\max}$ should obey $q\propto\omega_{\max}^{\tilde{d}/D_f}$. The dispersion relation obtained from $S(q,\omega)$ becomes $q\propto\omega_{\max}^{0.64\pm0.05}$, which is consistent with the value obtained from $\tilde{d}$ and D_f in Figs. 3(b) and 5(a). Figure 6(b) shows the rescaled plot of $S(q,\omega)$ of $d=3$ DLCA at $c=0.20$. In contrast to Fig. 6(a), plotted data in Fig. 6(b) are not fitted onto a single universal curve. The difference between Figs. 6(a) and 6(b) originates from whether the system shows a self-similarity or not. Our calculated results shown in Fig. 6(a) are in agreement with above theoretical predictions.

IV. CONCLUSIONS

In this paper we have performed large-scale simulations on cluster-cluster aggregations, which is known to be a successful model for the gel formation. The aggregates are formed on a square lattice and a simple cubic lattice with different particle concentrations. We have studied the density-density correlation function $g(r)$ for $d=3$ DLCA. At the lower concentration, self-similarities have been surely demonstrated from the calculated density-density correlation function $g(r)$. The fractal dimension D_f of the DLCA is numerically obtained, from the concentration dependence of the correlation length ξ, as $D_f\approx1.77$ in $d=3$, in agreement with previous studies. Vibrational densities of states $\mathcal{D}(\omega)$ are calculated for DLCA and RLCA models and their concentration dependence is clarified. From these calculations, the relationship between the structure of the cluster-cluster

aggregations and its vibrational dynamics has become clear. We have found that the frequency dependence of the DOS shows a power-law behavior such as $\mathcal{D}(\omega) \propto \omega^{\tilde{d}-1}$. The spectral dimensions $\tilde{d}$ on $d=3$ take the values $\tilde{d}=1.17 \pm 0.04$ for DLCA and $\tilde{d}=1.28 \pm 0.03$ for RLCA, respectively. These results show that DLCA and RLCA have different power-law dependences of the DOS. At higher particle concentrations c, the crossover from extended phonons to strongly localized excitations is clearly observed. At $c=0.10$, though the correlation length of the DLCA within which the fractality of the aggregate becomes relevant is short, the frequency regime where the DOS follows the power-law is quite large. This point remains to be clarified for future investigations. We have also investigated the frequency dependence of the dynamical structure factor $S(q,\omega)$ and its scaling properties for $d=3$ DLCA. For lower concentrations c, calculated results are fitted onto a single universal curve as shown in Fig. 6(a), revealing that the single-length scaling postulate is satisfied for $S(q,\omega)$. On the contrary, $S(q,\omega)$ is not rescaled with a single characteristic length scale for the system with higher concentrations c. This indicates that the self-similarity is an important factor for our results. We have demonstrated that computer simulations provide comprehensive results for the investigation of the dynamical properties of systems described by cluster-cluster aggregations [17].

ACKNOWLEDGMENTS

This work was supported in part by a Grant-in-Aid from the Japan Ministry of Education, Science, and Culture for Scientific Research in Priority Areas, Cooperative Phenomena in Complex Liquid. The authors thank the Supercomputer Center, Institute of Solid State Physics, University of Tokyo for the use of the facilities.

[1] T. Vicsek, *Fractal Growth Phenomena* (World Scientific, Singapore, 1989).
[2] A. Erzan, L. Pietronero, and A. Vespignani, Rev. Mod. Phys. **67**, 545 (1995).
[3] T. A. Witten and L. M. Sander, Phys. Rev. Lett. **47**, 1400 (1981).
[4] P. Meakin, Phys. Rev. Lett. **51**, 1119 (1983).
[5] M. Kolb, R. Botet, and R. Jullien, Phys. Rev. Lett. **51**, 1123 (1983).
[6] F. Family and D. P. Landau, *Kinetics of Aggregation and Gelation* (North-Holland, Amsterdam, 1984).
[7] M. Kolb and H. Herrmann, J. Phys. A **118**, L435 (1985).
[8] T. Nakayama, K. Yakubo, and R. L. Orbach, Rev. Mod. Phys. **66**, 381 (1994), and references therein.
[9] T. Terao and T. Nakayama, Phys. Rev. B **53**, R2918 (1996).
[10] S. Alexander and R. Orbach, J. Phys. (Paris) **43**, L625 (1982).
[11] R. Rammal and G. Toulouse, J. Phys. (Paris) **44**, L13 (1983).
[12] E. Courtens, R. Vacher, J. Pelous, and T. Woignier, Europhys. Lett. **6**, 245 (1988).
[13] R. Vacher, E. Courtens, G. Coddens, A. Heidemann, Y. Tsujimi, J. Pelous, and M. Foret, Phys. Rev. Lett. **65**, 1008 (1990).
[14] Y. Tsujimi, E. Courtens, J. Pelous, and R. Vacher, Phys. Rev. Lett. **60**, 2757 (1988).
[15] S. Alexander, E. Courtens, and R. Vacher, Physica A **195**, 286 (1993).
[16] E. Stoll, M. Kolb, and E. Courtens, Phys. Rev. Lett. **68**, 2472 (1992).
[17] A. Hasmy, E. Anglaret, M. Foret, J. Pelous, and R. Jullien, Phys. Rev. B **50**, 6006 (1994).
[18] R. Jullien and M. Kolb, J. Phys. A **17**, L639 (1984); P. Meakin and M. Muthukumar, J. Chem. Phys. **91**, 3212 (1989).
[19] According to previous studies, it is considered that the structure of base-catalyzed silica aerogels is described by DLCA, while that of neutrally catalyzed aerogels is more likely described by RLCA (see Ref. [17] and references therein).
[20] M. L. Williams and H. J. Maris, Phys. Rev. B **31**, 4508 (1985).
[21] T. Terao and T. Nakayama, Physica B **219&220**, 357 (1996).
[22] The value of α in Eq. (5) is taken to be $\alpha=-1/D_f$ in previous studies [17], in order to insure that the diffusion coefficient of aggregates varies with the inverse of their radius.
[23] A. Rahmani, C. Benoit, R. Jullien, G. Poussigue, and A. Sakout, J. Phys.: Condens. Matter **8**, 5555 (1996).
[24] E. Anglaret, A. Hasmy, E. Courtens, J. Pelous, and R. Vacher, Europhys. Lett. **28**, 591 (1994).